Combined a posteriori modelling-discretization error estimate for elliptic problems with variable coefficients

S. Repin*, T. Samrowski†, S. Sauter‡

Abstract

We consider linear elliptic problems with variable coefficients, which may sharply change values and have a complex behavior in the domain. For these problems, a new combined discretization-modeling strategy is suggested and studied. It uses a sequence of simplified models, which approximate coefficients with increasing accuracy. Boundary value problems generated by these simplified models are solved numerically, and the corresponding approximation errors are estimated by a posteriori estimates of the functional type. Modelling errors are also explicitly evaluated. An efficient numerical strategy is based upon balancing modelling and discretization errors, which provides an economical way of getting an approximate solution with an a priori given accuracy. Numerical tests demonstrate the reliability and efficiency of this adaptive numerical technology.

1 Introduction

We consider elliptic boundary value problems with rather complex behavior of the coefficients that form the corresponding differential operator. From the physical point of view, they can be regarded as models of a stationary diffusion with discontinuous, possibly, very *rough* diffusion coefficients. Certainly, there is a straightforward way of setting the corresponding approximate solutions, which consists of solving a problem on a sufficiently fine mesh that enables one to reproduce all the details of the diffusion coefficient and eliminate quadrature errors in the stiffness matrix coefficients. However, this is usually an expensive way. If solely a numerical solution with a certain guaranteed accuracy is required, then another strategy might be more efficient. It consists of two basic steps. First, the distribution of coefficients must be replaced by a simpler one. Then, the simplified model on a much coarser mesh should be solved. The control that the corresponding discretization error is below some given tolerance level can be obtained by applying guaranteed a posteriori estimates of the functional type. A guaranteed upper bound of the total error is determined as the sum of approximation and modelling errors and is computable, since the modelling error, which arises due to the replacement of the original problem by a simplified one, is also explicitly estimated. If the bound exceeds the desired tolerance, either the mesh should be refined (if the discretization error is essential) or the coefficient behavior must be modelled in more detail (if the modelling error is much larger than the discretization error). Hence, a *combined modelling-discretization* error estimation strategy is developed, in which the modelling E_{mod} and the discretization E_{disc} errors are properly balanced in accordance with the nature of the problem considered and the accuracy required.

Historically, the subject of a posteriori error estimation was mainly focused on the indication of discretization errors (e.g., see [3], [25], and references therein). In these cases, the error

*Steklov Institute, St.-Petersburg, Russia; e-mail: repin@pdmi.ras.ru

†Institut für Mathematik, Universität Zürich, Zürich, Switzerland; e-mail: tatiana.samrowski@math.uzh.ch

‡Institut für Mathematik, Universität Zürich, Zürich, Switzerland; e-mail: stas@math.uzh.ch

is measured by the quantity $\|u - u_h\|$, where u is the exact solution, u_h is the Galerkin approximation, and $\|\cdot\|$ is a certain norm associated with the problem. Most of the numerous publications, which are devoted to methods of estimating this quantity, can be combined into two main groups by the so-called residual method (see, e.g., [2], [3], [4], [5], [8], [11], [24], [25]) and the gradient averaging method (see, e.g., [6]).

In [13] - [22], a different approach to the a posteriori error control was suggested. In the framework of this approach, a posteriori estimates are derived by purely functional methods without attracting specific information on the approximating subspace and the numerical method used. As a result, the estimates contain no mesh dependent constants and are valid for any conforming approximation from the respective energy class. In the papers [21, 22], these properties have been used for analysis of modelling errors. Explicit and computable estimates of modelling errors related to dimension reduction models of diffusion type problems have been derived in [19, 20]. For more complicated plate models in the theory of linear elasticity, such type estimates have been recently derived in [16]. The problem of hierarchical modelling and dimension reduction has also been investigated in [7], [24], and [27]. The present paper is concerned with modelling errors of a different nature, which are not associated with the dimensional reduction but are stipulated by simplification of the coefficients.

The structure of the paper is as follows. In Section 2, we develop a combined modelling-discretization error estimation strategy for a class of elliptic boundary-value problems with variable coefficients. It is based upon guaranteed upper bounds of discretization and modelling errors, generated by simplified elliptic problems. Section 3 is devoted to a detailed description of control parameters, which is based upon combined modelling-discretization estimation. In Section 4, results of numerical tests are presented and discussed. Finally, conclusions are contained in Section 5.

2 A posteriori error estimation for the modelling and discretization error

2.1 Problem statement and notation

We consider the following elliptic problem

$$\begin{aligned} -\operatorname{div}(A\,\nabla u) &= f \quad \text{in } \Omega, \\ u &= 0 \quad \text{on } \partial\Omega, \end{aligned} \tag{1}$$

where Ω is a bounded domain in $\mathbb{R}^d$ $(d = 2, 3)$ with Lipschitz boundary $\partial\Omega$, $A(x)$ belongs to the set $\mathbb{R}^{d\times d}$ of $d \times d$ matrices with real coefficients, and I is the identity matrix. We assume that A is symmetric,

$$A(x) \in L^\infty(\Omega, \mathbb{R}^{d\times d}), \quad f \in L^2(\Omega),$$

and

$$c_1^2\,|\zeta|^2 \le A(x)\,\zeta \cdot \zeta \le c_2^2\,|\zeta|^2 \quad \text{for all } x \in \Omega \quad \text{and } \zeta \in \mathbb{R}^d. \tag{2}$$

Henceforth, the norm in $L^2(\Omega)$ is denoted by $\|u\|_\Omega$ and $\cdot$ means the scalar product of vectors. The notation $L^2(\Omega, \mathbb{R}^d)$ is used for vector-valued functions with components in $L^2(\Omega)$ and $\sigma(M)$ denotes the spectrum of $M \in \mathbb{R}^{d\times d}$. If the coefficients of M depend on x, then $\rho(M)$ denotes the maximum of the spectral radius, i.e., $\rho(M) := \sup\limits_{x\in\Omega} \max \sigma(M(x))$.

By $H(\Omega,\,\mathrm{div})$ we denote the subspace of $L^2(\Omega,\,\mathbb{R}^d)$ that contains vector-valued functions with square-integrable divergence, i.e.,

$$H\,(\Omega,\mathrm{div})\;:=\;\{q\in L^2\,(\Omega,\,\mathbb{R}^d)\;|\,\mathrm{div}\,q\in L^2\,(\Omega)\}.$$

It is a Hilbert space endowed with the scalar product

$$(p,\,q)_{\mathrm{div}}\;:=\int\limits_{\Omega}(p\cdot q\;+\;\mathrm{div}\,p\,\mathrm{div}\,q)$$

and the norm

$$\|q\|_{\mathrm{div}}\;:=\;(\|q\|^2_{\Omega}\;+\;\|\mathrm{div}\,q\|^2_{\Omega})^{1/2}.$$

For the functions in $L^2\,(\Omega,\,\mathbb{R}^d)$, we also use the norms

$$\|q\|_A\;:=\;\left(\int\limits_{\Omega}A\,q\;\cdot\;q\right)^{1/2}\tag{3}$$

and

$$\|q\|_{A^{-1}}\;:=\;\left(\int\limits_{\Omega}A^{-1}\,q\;\cdot\;q\right)^{1/2}.\tag{4}$$

The subspace of $H^1(\Omega)$ that consists of functions vanishing on $\partial\Omega$ is denoted by V_0.

We define a generalized solution of (1) as a function $u\in V_0$ that satisfies the integral identity

$$b\,(u,\,v)\;=\int\limits_{\Omega}f\,v,\quad\forall v\in V_0,\tag{5}$$

where $b\,(u,\,v):=\int\limits_{\Omega}A\,\nabla u\;\cdot\nabla v$ is the bilinear form generated by A. It is well known that the generalized solution u defined by (5) exists and is unique.

We consider a special class of such boundary value problems, which often arises in applications (e.g., in environmental modelling). Assume that the coefficients $a_{ij}(x)$ of the diffusion matrix A depend on x in a very complicated way. Then, the original problem becomes so complicated that solving it by standard methods may lead to an extremely high numerical cost. However, if only a certain (practically sufficient) accuracy is required, then solving the original (fully detailed) problem may be not the optimal strategy. If the modelling errors due to the simplification of data can be explicitly evaluated, then various simplified models can be used instead of the original one. In this paper, we show that the latter way is indeed efficient and in many cases it is possible to obtain a solution with a practically acceptable accuracy with the help of a simplified boundary value problem. For this purpose, we derive an a posteriori error estimate of the total error (which includes both discretization and modelling errors) and develop a solution strategy, based on the interplay between the choice of the model and the approximation subspace.

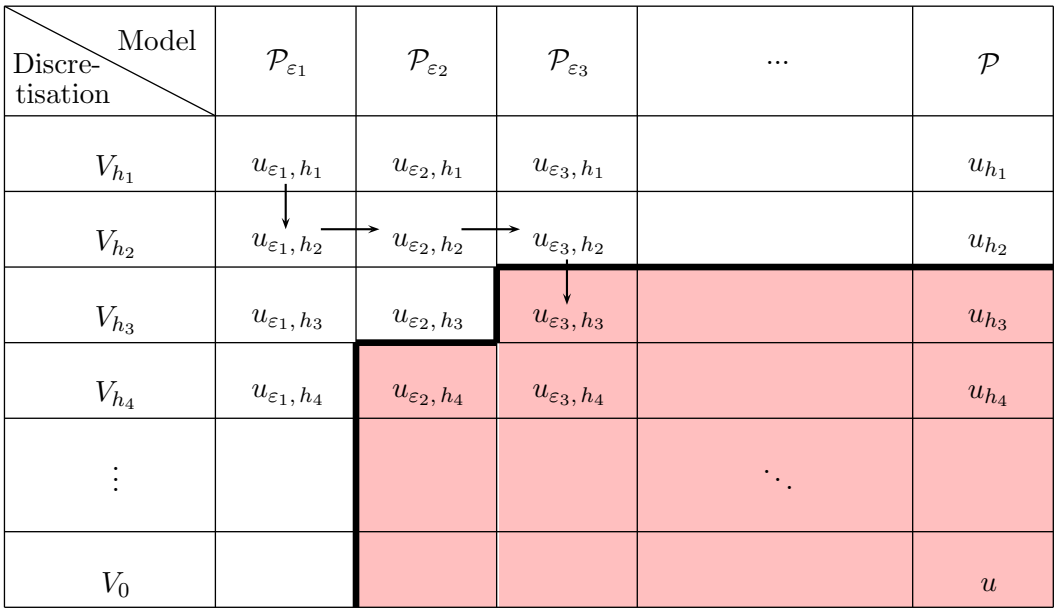

Figure 1: *Combined adaptive modelling-discretization strategy*

2.2 Combined modelling-discretization error estimation

The idea of the *combined modelling-discretization error estimation (MD**E**)* strategy can be explained with the help of a diagram exposed in Figure 1. Assume that the original problem (1) must be solved with some guaranteed accuracy δ. This can be achieved not only by computing the solution of the "given" problem, but also by employing some simplified problems $\mathcal{P}_{\varepsilon_1}$, $\mathcal{P}_{\varepsilon_2}$, ..., $\mathcal{P}_{\varepsilon_k}$, using a dense sequence of finite dimensional subspaces $V_{h_1} \subset V_{h_2} ... \subset V_{h_k}$.

The last column of the table in Figure 1 reflects the classical mesh adaptation procedure, in which finite dimensional subspaces are refined until the corresponding approximate solution becomes sufficiently accurate (all functions whose deviations from u are less than δ belong to the zone lying below the bold line). In the last column, the first approximate solution having the desired accuracy is u_{h_3}. However, a procedure based purely on numerical discretization may be suboptimal by several reasons. For example, if the coefficients of a differential equation have a complicated structure, then well known difficulties with exact quadratures may arise. Moreover, the resolution of zones with jumping coefficients may lead to geometrical difficulties and require a large number of additional nodes (elements, degrees of freedoms). This way of doing may generate very large systems of linear equations (in particular, for 3D problems). However, if we need a solution with a moderate accuracy that belongs to the shaded zone (which is a typical engineering situation), then more economical ways exist. In particular, we can use the simplified model $\mathcal{P}_{\varepsilon_3}$ (whose solution in the space V_{h_3} possesses the same order of accuracy) or a simpler model $\mathcal{P}_{\varepsilon_2}$. These observations suggest the idea that the optimal strategy should be based on the combined modelling-discretization strategy MD**E**:

In the MD**E** strategy, we start with the coarsest model $\mathcal{P}_{\varepsilon_1}$, which is solved on V_{h_1}. By the combined modelling-discretization error majorant (see Theorem 2.1), the total error associated with u_{ε_1,h_1} is estimated by the sum of the corresponding modelling error (denoted by $E^{\varepsilon_1}_{mod}$) and the discretization error ($E^{\varepsilon_1,-\log_2 h_1}_{disc}$). Assume that the tolerance level has not been achieved (i.e., the overall error exceeds the given tolerance δ) and $E^{\varepsilon_1}_{mod} < \alpha\, E^{\varepsilon_1,-\log_2 h_1}_{disc}$,

where α is a positive real number that balances values of approximation and modelling errors (in the numerical tests, we set $\alpha = 0.4$). Then, the subspace V_{h_1} should be refined, and we pass to V_{h_2}. If $E^{\varepsilon_1}_{mod} \geq \alpha\, E^{\varepsilon_1,\,-\log_2 h_1}_{disc}$, then an improved model should be chosen (we pass to $\mathcal{P}_{\varepsilon_2}$). With this strategy, an economical way to find a desirable approximation, e.g., $u_{\varepsilon_3,\,h_3}$, is marked by arrows. It is worth mentioning that approximate solutions and their components (e.g., fluxes) computed on some steps of the algorithm can further be used on subsequent steps as good initial guesses for iterative solvers.

2.3 Combined error majorant

Instead of the exact problem (5) we consider the following simplified one: Find $u_\varepsilon \in V_0$ such that

$$b_\varepsilon(u_\varepsilon,\, v) \;:=\; \int\limits_\Omega A_\varepsilon\, \nabla u_\varepsilon \cdot \nabla v \;=\; \int\limits_\Omega f\, v \quad \text{for all } v \in V_0, \tag{6}$$

where $A_\varepsilon \in L^\infty(\Omega,\, \mathbb{R}^{d\times d})$ is a certain approximation of A. We assume that the parameter ε characterizes the difference between A and A_ε, so that A_ε increasingly approximate A as ε tends to zero. Also, we assume that for any ε, the matrix A_ε is positive definite and

$$c^2_{1\varepsilon}\,|\zeta|^2 \;\leq\; A_\varepsilon(x)\,\zeta \cdot \zeta \;\leq\; c^2_{2\varepsilon}\,|\zeta|^2 \quad \text{for all } x \in \Omega \quad \text{and } \zeta \in \mathbb{R}^d. \tag{7}$$

Let $\mathcal{T}_h$ be a simplicial mesh with mesh size h. We define the following spaces:

- $S_h := \{u \in C^0(\overline{\Omega}) \big|$ for any $\tau \in \mathcal{T}_\mathrm{h}$: $\mathrm{u}|_\tau$ is an affine function$\}$;
- $S_{h,0} := S_h \cap V_0$;
- $S^2_h := S_h \times S_h$.

The problem (6) is solved numerically. We find the corresponding Galerkin solution $u_{\varepsilon,h} \in S_{h,0}$ that satisfies the relation

$$b_\varepsilon(u_{\varepsilon,h},\, v_h) \;:=\; \int\limits_\Omega A_\varepsilon\, \nabla u_{\varepsilon,h} \cdot \nabla v_h \;=\; \int\limits_\Omega f\, v_h \quad \text{for all } v_h \in S_{h,0}. \tag{8}$$

In order to estimate the *discretization* error $\|\nabla(u_\varepsilon - u_{\varepsilon,h})\|_{A_\varepsilon}$, we use a posteriori error estimates of the functional type (see [12] - [18], [21, 22] and the references therein), which in our case takes the form

$$\|\nabla(u_\varepsilon - u_{\varepsilon,h})\|^2_{A_\varepsilon} \leq \mathcal{M}^2_\Omega(u_{\varepsilon,h}, y,\, \beta) := (1+\beta)\|A_\varepsilon\, \nabla u_{\varepsilon,\,h} - y\|^2_{A^{-1}_\varepsilon} + \\ + \left(1 + \frac{1}{\beta}\right) C^2_\Omega \|\mathrm{div}\, y + f\|^2_\Omega. \tag{9}$$

Here, $\mathcal{M}_\Omega(u_{\varepsilon,h},\, y,\, \beta)$ is the a posteriori error majorant, y is an arbitrary vector-valued function from $H(\Omega, \mathrm{div})$, β is an arbitrary positive number, and $C_\Omega := \frac{1}{c^2_{1\varepsilon}} C^2_{F\Omega}$, where $C_{F\Omega}$ is the Friedrichs' constant for the domain Ω, defined by

$$C_{F\Omega} := \sup_{w \in V_0 \setminus \{0\}} \frac{\|w\|_\Omega}{\|\nabla w\|_\Omega}.$$

For the class of problems under consideration, a combined modelling-discretization a posteriori estimate of the total error $\|\nabla(u - u_{\varepsilon,h})\|_A$ is presented below.

Theorem 1 *For the total error* $\|\nabla(u - u_{\varepsilon,h})\|_A$ *it holds*

$$\|\nabla(u - u_{\varepsilon,h})\|_A \le E_{disc}^{\varepsilon,h} + E_{mod}^{\varepsilon}. \tag{10}$$

In (10), $E_{disc}^{\varepsilon,h}$ *and* E_{mod}^{ε} *represent the discretization and modelling parts of the error, respectively, which are defined and estimated as follows:*

$$E_{disc}^{\varepsilon,h} := \|\nabla(u_\varepsilon - u_{\varepsilon,h})\|_A \le \kappa_1 \mathcal{M}_\Omega(u_{\varepsilon,h}, y, \beta), \tag{11}$$

$$E_{mod}^{\varepsilon} := \|\nabla(u - u_\varepsilon)\|_A \le \kappa_2 \big(\mathcal{M}_\Omega^2(u_{\varepsilon,h}, y, \beta) + \|\nabla u_{\varepsilon,h}\|_{A_\varepsilon}^2\big)^{1/2} \tag{12}$$

where $\Lambda_\varepsilon := A_\varepsilon^{-1/2} A A_\varepsilon^{-1/2}$, $\kappa_1^2 = 1 + \rho(\Lambda_\varepsilon - I)$, *and* $\kappa_2^2 = \rho(\Lambda_\varepsilon + \Lambda_\varepsilon^{-1} - 2I)$.

Proof: By the triangle inequality, we obtain

$$\|\nabla(u - u_{\varepsilon,h})\|_A \le \|\nabla(u_\varepsilon - u_{\varepsilon,h})\|_A + \|\nabla(u - u_\varepsilon)\|_A = E_{disc}^{\varepsilon,h} + E_{mod}^{\varepsilon}. \tag{13}$$

We estimate the term $E_{disc}^{\varepsilon,h} = \|\nabla(u_\varepsilon - u_{\varepsilon,h})\|_A$, as follows:

$$\begin{aligned}
\Big(E_{disc}^{\varepsilon,h}\Big)^2 &= \|\nabla(u_\varepsilon - u_{\varepsilon,h})\|_{A_\varepsilon}^2 + \int_\Omega (A - A_\varepsilon)\,\nabla(u_\varepsilon - u_{\varepsilon,h}) \cdot \nabla(u_\varepsilon - u_{\varepsilon,h}) \\
&= \|\nabla(u_\varepsilon - u_{\varepsilon,h})\|_{A_\varepsilon}^2 + \int_\Omega (\Lambda_\varepsilon - I) A_\varepsilon^{1/2} \nabla(u_\varepsilon - u_{\varepsilon,h}) \cdot A_\varepsilon^{1/2}\,\nabla(u_\varepsilon - u_{\varepsilon,h}) \\
&\le \big(1 + \rho(\Lambda_\varepsilon - I)\big)\|\nabla(u_\varepsilon - u_{\varepsilon,h})\|_{A_\varepsilon}^2.
\end{aligned}$$

Since the last norm is estimated by (9), we arrive at (11). To estimate the term E_{mod}^{ε}, we note that

$$0 = b\,(u - u_\varepsilon,\, v) + (b - b_\varepsilon)\,(u_\varepsilon,\, v), \qquad \forall\, v \in V_0,$$

and choose $v = u - u_\varepsilon$. Then,

$$\begin{aligned}
(E_{mod}^{\varepsilon})^2 = \|\nabla(u - u_\varepsilon)\|_A^2 &= b\,(u - u_\varepsilon,\, u - u_\varepsilon) = (b_\varepsilon - b)(u_\varepsilon,\, u - u_\varepsilon) \\
&= \int_\Omega (A_\varepsilon - A)\,\nabla u_\varepsilon \cdot \nabla(u - u_\varepsilon).
\end{aligned}$$

By the Hölder inequality, we find that

$$\|\nabla(u - u_\varepsilon)\|_A^2 \le \left(\int_\Omega (A_\varepsilon - A)\,A^{-1}(A_\varepsilon - A)\nabla u_\varepsilon \cdot \nabla u_\varepsilon\right)^{1/2} \|\nabla(u - u_\varepsilon)\|_A.$$

Hence,

$$\begin{aligned}
\|\nabla(u - u_\varepsilon)\|_A^2 &\le \int_\Omega (A_\varepsilon - A)A^{-1}(A_\varepsilon - A)\nabla u_\varepsilon \cdot \nabla u_\varepsilon \\
&= \int_\Omega (\Lambda_\varepsilon + \Lambda_\varepsilon^{-1} - 2I) A_\varepsilon^{1/2} \nabla u_\varepsilon \cdot A_\varepsilon^{1/2} \nabla u_\varepsilon \le \rho\,(\Lambda_\varepsilon + \Lambda_\varepsilon^{-1} - 2I)\,\|\nabla u_\varepsilon\|_{A_\varepsilon}^2.
\end{aligned}$$

Note that

$$\int_\Omega A_\varepsilon \nabla u_{\varepsilon,h} \cdot \nabla u_{\varepsilon,h} + \int_\Omega A_\varepsilon \nabla (u_\varepsilon - u_{\varepsilon,h}) \cdot \nabla (u_\varepsilon - u_{\varepsilon,h}) =$$

$$= \int_\Omega A_\varepsilon \nabla u_\varepsilon \cdot \nabla u_\varepsilon - 2 \int_\Omega A_\varepsilon \nabla u_{\varepsilon,h} \cdot \nabla (u_\varepsilon - u_{\varepsilon,h}) = \|\nabla u_\varepsilon\|^2_{A_\varepsilon}$$

and, therefore,

$$\|\nabla (u - u_\varepsilon)\|^2_A \le \rho \, (\Lambda_\varepsilon + \Lambda_\varepsilon^{-1} - 2I) \big(\|\nabla u_\varepsilon - \nabla u_{\varepsilon,h}\|^2_{A_\varepsilon} + \|\nabla u_{\varepsilon,h}\|^2_{A_\varepsilon} \big). \tag{14}$$

Finally, we estimate the first term of (14) by the error majorant and get

$$\|\nabla (u - u_\varepsilon)\|_A \le \rho^{1/2} (\Lambda_\varepsilon + \Lambda_\varepsilon^{-1} - 2I) \big(\mathcal{M}^2_\Omega (u_{\varepsilon,h},\, y,\, \beta) + \|\nabla u_{\varepsilon,h}\|^2_{A_\varepsilon} \big)^{1/2}, \tag{15}$$

which yields (12). □

Remark 1 *We note that the error $\|\nabla (u - u_{\varepsilon,h})\|_A$ can be directly estimated by the error majorant analogously to (9), in which the first term is generated by the original matrix A (instead of A_ε^{-1}). However, this way has two essential drawbacks. First, computations related to the majorant with A may require complicated integration procedures (especially if the problem contains fine structures). For this reason, it is much simpler to find a suitable y and evaluate the majorant if A_ε instead of A. Another point is that the estimate (10) includes two meaningful quantities (discretization and modelling errors). They are explicitly estimated by (11) and (12) what allows us to balance these errors with the help of an adaptive method described in Section 2.2.*

Remark 2 *From (10) it follows that*

$$\|\nabla (u - u_{\varepsilon,h})\|_A \le (\kappa_1 + \kappa_2) \mathcal{M}_\Omega (u_{\varepsilon,h},\, y,\, \beta) + \kappa_2 \|\nabla u_{\varepsilon,h}\|_{A_\varepsilon}. \tag{16}$$

It is easy to see that if $A = A_\varepsilon$, then $\Lambda_\varepsilon = \Lambda_\varepsilon^{-1} = I$, and $\kappa_1 = 1$, $\kappa_2 = 0$. In this case, the term related to the modelling error vanishes and the right hand side of (10) is completely determined by the discretization error.

If A and A_ε are diagonal matrices, then $\Lambda_\varepsilon = \{\lambda^\varepsilon_{ij}\}$ is also diagonal and $\lambda^\varepsilon_{ii} = \frac{a_{ii}}{a^\varepsilon_{ii}}$. In this case,

$$\kappa_1^2 \le 1 + |\Lambda_\varepsilon - I| = \quad 1 + \sup_{x \in \Omega} \max_{i=1,\dots,d} \frac{|a_{ii}(x) - a^\varepsilon_{ii}(x)|}{a^\varepsilon_{ii}(x)}, \tag{17}$$

$$\kappa_2^2 \le |\Lambda_\varepsilon + \Lambda_\varepsilon^{-1} - 2I| = \quad \sup_{x \in \Omega} \max_{i=1,\dots,d} \frac{(a_{ii}(x) - a^\varepsilon_{ii}(x))^2}{a_{ii}(x)\, a^\varepsilon_{ii}(x)}. \tag{18}$$

Suppose the error $|a_{ii} - a^\varepsilon_{ii}|_{L^\infty(\tilde\omega)} \le \varepsilon_{\tilde\omega}$ on local subregions $\tilde\omega$ is known in an a priori way. Such a situation arises if the coefficients involve uncertainties generated by, e.g., experimental data or errors of numerical integration. We see that κ_2 (more precisely: local versions thereof) is proportional to ε, and it is not difficult to compute this constant. Since E^ε_{mod} is bounded from below by the quantity $\kappa_2 \|\nabla u_{\varepsilon,h}\|_{A_\varepsilon}$ (which is easily computable if $u_{\varepsilon,h}$ is known), we obtain a bound for the overall accuracy. Assume that the tolerance level δ is significantly smaller than this quantity. In this situation, we conclude that the corresponding model (with uncertain data) cannot provide a solution within the desired accuracy and the analysis of the approximation

error is superfluous. In the discretiztion-modeling adaptive method, the value of $\kappa_2\|\nabla u_{\varepsilon,h}\|_{A_\varepsilon}$ *is also important. Since the evaluation of this value is much cheaper than the minimization of* $\mathcal{M}_\Omega(u_{\varepsilon,h},\, y,\, \beta)$ *w.r.t.* y*, it is recommended to first compute the term* $\kappa_2\|\nabla u_{\varepsilon,h}\|_{A_\varepsilon}$*. If it exceeds* δ*, then we see that it is necessary to consider a finer model avoiding computations related to* $\mathcal{M}_\Omega(u_{\varepsilon,h},\, y,\, \beta)$*.*

3 Evaluation of the error estimator

3.1 Sequence of simplified models

Henceforth, we assume that the diffusion coefficient A is piecewise constant, Ω is decomposed into connected disjoint subsets ω_i, $0 \le i \le q$ (called "inclusions"). By $\mathcal{H}$ and γ we denote the sets of all inclusions and their interfaces, respectively, i.e.,

$$\mathcal{H} := \{\omega_i :\, 0 \le i \le q\} \quad \text{and} \quad \gamma := \bigcup_{\omega\in\mathcal{H}} \partial\omega.$$

A *sequence of resolutions* $\widetilde{\mathcal{H}}_j$, $j = 0, 1, \ldots, J$, for the inclusions from $\mathcal{H}$ (illustrated in Figure 2) will be constructed subject to the following conditions:

1. $\widetilde{\mathcal{H}}_0 = \{\Omega\}$.
2. $\widetilde{\mathcal{H}}_j = \left\{\widetilde{\omega}_k^j :\, 0 \le k \le \tilde{q}_j\right\}$ is a disjoint partitioning of Ω, i.e.,
   (a) all $\widetilde{\omega}^j \in \widetilde{\mathcal{H}}_j$ are open subsets of Ω,
   (b) $\overline{\Omega} = \overline{\bigcup_{\widetilde{\omega}\in\widetilde{\mathcal{H}}_j} \widetilde{\omega}}$,
3. The final level $\widetilde{\mathcal{H}}_J$ equals $\mathcal{H}$ or is a refinement of $\mathcal{H}$, i.e.,

$$\forall\, \widetilde{\omega}^J \in \widetilde{\mathcal{H}}_J \quad \exists \omega \in \mathcal{H} :\, \widetilde{\omega}^J \subset \omega\,.$$

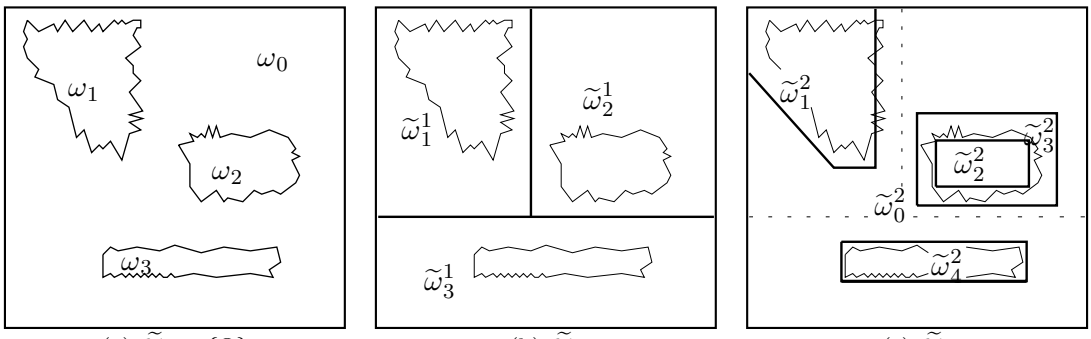

(a) $\widetilde{\mathcal{H}}_0 = \{\Omega\}$ (b) $\widetilde{\mathcal{H}}_1$ (c) $\widetilde{\mathcal{H}}_2$

Figure 2: *Example of the first three refinements in the sequence of resolutions of the inclusions*

Further we define simplified coefficients A_ε, which are constant on every $\widetilde{\omega}^l \in \widetilde{\mathcal{H}}_l$, as a suitable average of A. We use

$$\widetilde{\mathcal{H}}_{\widetilde{\omega}^l} := \{\omega \in \mathcal{H} :\, |\omega \cap \widetilde{\omega}^l| > 0\}$$

for the "influence region" of some $\widetilde{\omega}^l$ and denote by $\#\widetilde{\mathcal{H}}_{\widetilde{\omega}^l}$ the cardinality of $\widetilde{\mathcal{H}}_{\widetilde{\omega}^l}$. Basic averaging strategies are then given by

1) $A_\varepsilon|_{\widetilde{\omega}^l} := \frac{1}{\#\widetilde{\mathcal{H}}_{\widetilde{\omega}^l}} \sum_{i=0}^{\#\widetilde{\mathcal{H}}_{\widetilde{\omega}^l}} A|_{w_i}$, i.e., the arithmetic mean for $\widetilde{\mathcal{H}}_l$;

2) $A_\varepsilon|_{\widetilde{\omega}^l} := \left(\frac{1}{\#\widetilde{\mathcal{H}}_{\widetilde{\omega}^l}} \sum_{i=0}^{\#\widetilde{\mathcal{H}}_{\widetilde{\omega}^l}} (A|_{w_i})^{-1} \right)^{-1}$, i.e., the harmonic mean for $\widetilde{\mathcal{H}}_l$;

3) $A_\varepsilon|_{\widetilde{\omega}^l} := \frac{1}{|\widetilde{\omega}^l|} \int_{\widetilde{\omega}^l} A$, i.e., the arithmetic integral mean for $\widetilde{\mathcal{H}}_l$;

4) $A_\varepsilon|_{\widetilde{\omega}^l} := \left(\frac{1}{|\widetilde{\omega}^l|} \int_{\widetilde{\omega}^l} A^{-1} \right)^{-1}$, i.e., the harmonic integral mean for $\widetilde{\mathcal{H}}_l$.

From the literature (cf. [9], Chapter 8) it is known that for fine periodic structures the best averaging strategy is the harmonic integral mean.

3.2 Computation of the majorant

To estimate the errors $E^{\varepsilon,h}_{disc}$ and E^{ε}_{mod}, we need to evaluate the term $\mathcal{M}^2_\Omega(u_{\varepsilon,h}, y, \beta)$ (cf. Theorem 1) for a proper flux approximation y and a parameter β. The questions, how to choose β and how to compute the flux approximation y from the discrete solution $u_{\varepsilon_l,h}$, have already been discussed in the literature (e.g., see [12, 13, 14, 17, 18, 23, 26]). Below we briefly discuss the application of these methods to our case. We emphasize that Theorem 1 implies that any choice $(\beta, y) \subset \mathbb{R} \times H(\Omega, \mathrm{div})$ in the error majorant results in an upper bound of the error. However, sharp estimates require a proper choice of these quantities and a reasonable strategy, which we will introduce in the following, has to balance the extra computational cost with the benefit of sharper estimates.

If A, A_ε, f, and C_Ω are known, then the squared majorant $\mathcal{M}^2_\Omega(u_{\varepsilon,h}, y, \beta)$ is a quadratic functional. Our goal is to find some $y_h \in S^2_h$ and $\beta \in \mathbb{R}$ such that $\mathcal{M}^2_\Omega(u_{\varepsilon,h}, y_h, \beta)$ is close to the minimum over $y \in H(\Omega, \mathrm{div})$ and $\beta \in \mathbb{R}$. For the corresponding iterative algorithm (minimization with respect to β is a simple algebraic problem), we introduce the following notation:

For every vertex ξ of $\mathcal{T}_h$, denote by $\mathcal{P}_\xi := \{\tau \in \mathcal{T}_h : \xi \in \overline{\tau}\}$ the neighboring elements, by $\omega_\xi := \overline{\bigcup_{\tau \in \mathcal{P}_\xi} \tau}$ the patch of this vertex and define $y^{(0)}_h \in S^2_h$ implicitly from the patchwise flux averaging by the nodal condition

$$y^{(0)}_h(\xi) := \frac{1}{|\omega_\xi|} \int_{\omega_\xi} A_\varepsilon \nabla u_{\varepsilon,h}. \tag{19}$$

For all vertices ξ_j, $1 \le j \le N$, let $S_j := \mathrm{span}\{(b_j, 0), (0, b_j)\} \subset S_h$ denote the usual nodal basis for S_h and let $\mathcal{M}^2_{\Omega,\omega_{\xi_j}}(u_{\varepsilon,h}, y_h, \beta)$ be the contribution of the patch ω_{ξ_j} to the majorant $\mathcal{M}^2_\Omega(u_{\varepsilon,h}, y_h, \beta)$.

Algorithm 1 (global minimization of the error majorant):

Set $y_h^{(0)}(\xi) = \frac{1}{|\omega_\xi|}\int_{\omega_\xi} A_\varepsilon \nabla u_{\varepsilon,h}$ and $\beta^{(0)} = \frac{C_\Omega \|\mathrm{div}\, y_h^{(0)} + f_h\|_\Omega}{\|A_\varepsilon \nabla u_{\varepsilon,h} - y_h^{(0)}\|_{A_\varepsilon^{-1}}}$

Choose ν_{max}

For $\nu = 1$ to ν_{max} do begin

$$\begin{aligned} y_h^{(\nu)} &= \operatorname*{argmin}_{v\in S_h^2} \mathcal{M}_\Omega^2(u_{\varepsilon,h}, v, \beta^{(\nu-1)}) \\ \beta^{(\nu)} &= \frac{C_\Omega \|\mathrm{div}\, y_h^{(\nu)} + f_h\|_\Omega}{\|A_\varepsilon \nabla u_{\varepsilon,h} - y_h^{(\nu)}\|_{A_\varepsilon^{-1}}} \end{aligned} \tag{20}$$

end

Calculate $\mathcal{M}_\Omega^2(u_{\varepsilon,h}, y_h^{(\nu_{max})}, \beta^{(\nu_{max})})$

We note that the global minimization requires the generation and solution of a linear system of dimension $2\,N$. On the one hand, we expect that the computational cost are of the same order as the cost for computing $u_{\varepsilon,h}$. On the other hand, one could save memory (at the expense of less sharp estimates) if (20) is replaced by a few steps of a Gauss-Seidel type iteration (21):

Algorithm 2 (local minimization of the error majorant):

Set $y_h^{(0)}(\xi) = \frac{1}{|\omega_\xi|}\int_{\omega_\xi} A_\varepsilon \nabla u_{\varepsilon,h}$ and $\beta^{(0)} = \frac{C_\Omega \|\mathrm{div}\, y_h^{(0)} + f_h\|_\Omega}{\|A_\varepsilon \nabla u_{\varepsilon,h} - y_h^{(0)}\|_{A_\varepsilon^{-1}}}$

Choose ν_{max} and ι_{max}

For $\nu = 1$ to ν_{max} do begin

Set $\gamma_N^{(0)} = y_h^{(\nu-1)}$

For $i = 1$ to ι_{max} do begin

$$\begin{aligned} &\gamma_0^{(i)} = \gamma_N^{(i-1)} \\ &\text{For } j = 1 \text{ to } N \text{ do begin} \\ &\quad v_j = \operatorname*{argmin}_{v\in S_j^2} \mathcal{M}^2_{\Omega,\omega_{\xi_j}}(u_{\varepsilon,h},\, \gamma_{j-1}^{(i)} + v, \beta^{(\nu-1)}) \\ &\quad \gamma_j^{(i)} = \gamma_{j-1}^{(i)} + v_j \\ &\text{end} \end{aligned} \tag{21}$$

end

Set $y_h^{(\nu)} = \gamma_N^{(\iota_{max})}$ and $\beta^{(\nu)} = \frac{C_\Omega \|\mathrm{div}\, y_h^{(\nu)} + f_h\|_\Omega}{\|A_\varepsilon \nabla u_{\varepsilon,h} - y_h^{(\nu)}\|_{A_\varepsilon^{-1}}}$

end

Calculate $\mathcal{M}_\Omega^2(u_{\varepsilon,h}, y_h^{(\nu_{max})}, \beta^{(\nu_{max})})$

4 Numerical results

In this section, we demonstrate the performance of the combined MD**E** strategy for the case of a linear diffusion problem with a discontinuous, piecewise constant diffusion coefficient, which has rather complex interfaces separating its discontinuities.

In the following experiments, we consider the domain $\Omega = (0,\,1)^2$ with an inclusion ω_1 (c.f. Figure 3). We choose

$$A|_{\omega_1} = 2\,I \quad \text{and} \quad A|_{\omega_0} = I \tag{22}$$

and note that the exact structure of A can be resolved on the uniform mesh with $h = 1/32$.

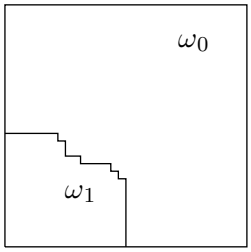

Figure 3: *Unit square with the inclusion* ω_1

The right-hand side of the diffusion equation is given by

$$f(x,\,y) = 2x\,(1-x) + 2y\,(1-y). \tag{23}$$

Remark 3 *If one solves this diffusion problem with standard* $\mathbb{P}_1$ *finite elements on some coarse mesh which does not resolve the discontinuities in A, the quadrature for setting up the stiffness matrix either becomes very expensive (depending on the "roughness" of the interface) or prohibitive inaccurate. Note that our numerical example has mainly the purpose to illustrate the behavior and sharpness of our modelling-discretization error estimator as well as the proper selection of the control parameters and* ***not*** *its application to three-dimensional problems with very many rough interfaces – this will be the topic of further research.*

We construct a series of Models 1-4, in which Model 1 is the coarsest model and Model 4 is the finest one. The corresponding diffusion matrices are denoted by A_{ε_1} and A_{ε_4}, respectively. They are defined on the corresponding resolution levels $\widetilde{\mathcal{H}}_1$ to $\widetilde{\mathcal{H}}_4$ (cf. Figure 4) by using the harmonic averaging

$$A_{\varepsilon_i}|_{\widetilde{\omega}_j^i} := \left(\frac{1}{|\widetilde{\omega}_j^i|} \int\limits_{\widetilde{\omega}_j^i} A^{-1} \right)^{-1}, \qquad \widetilde{\omega}_j^i \in \widetilde{\mathcal{H}}_i,\ i = 1, ..., 4,\ j = 0, ..., 4. \tag{24}$$

We note that the exact structure of A_{ε_1} can be resolved on the very coarse mesh with $h = 2^{-1}$, in the case of A_{ε_2} it can be exactly resolved with $h = 2^{-3}$ and in the case of A_{ε_3} and A_{ε_4} - with $h = 2^{-4}$ and $h = 2^{-5}$ correspondingly. Instead of the exact problem (1), we numerically solve its simplified counterparts associated with different resolution levels and estimate the approximation errors by the a posteriori error majorants (see Theorem 1).

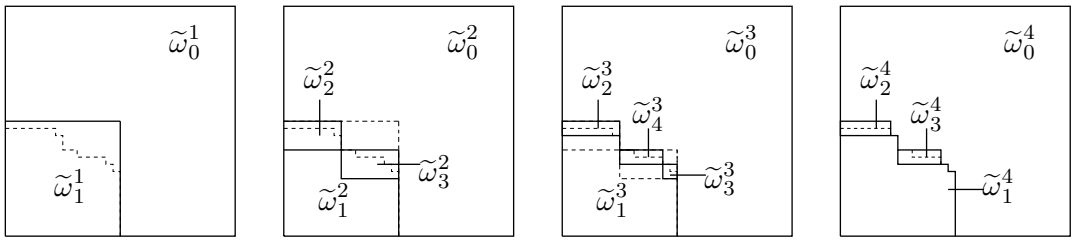

(a) $\widetilde{\mathcal{H}}_1$ (b) $\widetilde{\mathcal{H}}_2$ (c) $\widetilde{\mathcal{H}}_3$ (d) $\widetilde{\mathcal{H}}_4$

Figure 4: *Hierarchy of simplified nodels.*

First we present results of computer simulation that demonstrate the efficiency of the minimization strategies (19)-(21).

Test 1.1 We select Model 1, set $h = 2^{-5}$, use a GMRES-Solver to find an approximate solution, and estimate the total error by the combined modelling-discretization error majorant $\mathscr{M}$ verified in Section 3.2 and defined here by

$$\mathscr{M} := E_{disc}^{\varepsilon,h} + \left(\widetilde{E_{mod}^{\varepsilon}}^{\,2} + \widehat{E_{mod}^{\varepsilon}}^{\,2}\right)^{1/2}, \tag{25}$$

where

$$\widetilde{E_{mod}^{\varepsilon}} := \kappa_2^{1/2}\,\mathcal{M}_\Omega(u_{\varepsilon,h},\, y,\, \beta) \quad \text{and} \quad \widehat{E_{mod}^{\varepsilon}} := \kappa_2^{1/2}\,\|\nabla u_{\varepsilon,h}\|_{A_\varepsilon}$$

(cf. (12)), by using the approximative (local) and global minimization strategy (see Section 3.2).

The parameters of the local minimization algorithm are ι_{max} and ν_{max}. In our first test we set $\nu_{max} = 1$ and vary ι_{max} from $0 - 9$. The first line of Table 1 corresponds to the case in which y is constructed by simple flux averaging (19). Table 1 shows that $\iota_{max} = 3$ is enough for getting accurate values of $\mathscr{M}$ and further iterations ($\iota_{max} = 6$ to $\iota_{max} = 9$) do not significantly improve it. Similar tests with the other models show the same results.

ι_{max}	β_1	E_{disc}	$\widetilde{E_{mod}}$	$\widehat{E_{mod}}$	$\mathscr{M}$	t, $[sec]$
0	1.924	0.0299	0.0032	0.0148	0.0450	1.6
3	0.568	0.0146	0.0022	0.0148	0.0296	6.85
6	0.517	0.0139	0.0022	0.0148	0.0289	15.41
9	0.504	0.0137	0.0022	0.0148	0.0287	20.75

Table 1: *The total error majorant and CPU time in seconds required for optimization of the flux function in the case of Model 1 for* $\nu_{max} = 1$.

Test 1.2: In this series of numerical experiments we set $\iota_{max} = 3$ and increase the parameter ν_{max}. The corresponding results are presented in Table 2. They demonstrate that increasing of ν_{max} does not significantly improve the majorant. For this reason by using the approximative (local) minimization strategy from Algorithm 2, it is sufficient to choose $\iota_{max} = 3$ and $\nu_{max} = 1$.

Test 1.3: Now we demonstrate the efficiency of the global minimization strategy. We solve the four selected approximate models on the meshes with $h = 2^{-5}, 2^{-6}, 2^{-7}$ and evaluate the total error majorant by using of the local (with $\iota_{max} = 3$ and $\nu_{max} = 1$) and global

ν_{max}	$\beta_{\nu_{max}}$	E_{disc}	$\widetilde{E_{mod}}$	$\widehat{E_{mod}}$	$\mathscr{M}$	t, $[sec]$
1	0.568	0.0146	0.0022	0.0148	0.0296	6.85
2	0.511	0.0139	0.0022	0.0148	0.0289	14.45
3	0.498	0.0138	0.0022	0.0148	0.0287	22.57

Table 2: *The total error majorant and CPU time in seconds required for optimization of the flux function in the case of Model 1 for* $\iota_{max} = 3$.

(with $\nu_{max} = 1$) minimization strategy. We denote these error majorants by $\mathscr{M}^{loc}$ and $\mathscr{M}^{glob}$ correspondingly. Table 3 presents the results. As expected the global strategy provides the exacter majorants and should be preferred if the technical ability allows the treatment of large systems of equations. That is why for our subsequent tests, we choose the global minimization strategy and solve the linear systems with a PARDISO-solver from http://www.pardiso-project.org/download/academic.cgi.

$-\log_2 h$	Model 1		Model 2		Model 3		Model 4	
	$\mathscr{M}^{loc}$	$\mathscr{M}^{glob}$	$\mathscr{M}^{loc}$	$\mathscr{M}^{glob}$	$\mathscr{M}^{loc}$	$\mathscr{M}^{glob}$	$\mathscr{M}^{loc}$	$\mathscr{M}^{glob}$
5	0.0296	0.0282	0.0259	0.0243	0.0246	0.0230	0.0240	0.0224
6	0.0240	0.0226	0.0209	0.0192	0.0195	0.0175	0.0182	0.0171
7	0.0214	0.0203	0.0185	0.0168	0.0172	0.0151	0.0158	0.0147

Table 3: *Comparison of the total error majorant calculated by using of different minimization strategies.*

Now we present tests that demonstrate the performance of the MD**E** strategy.

Test 2.1: To quantify the efficiency of the calculation of the error majorant, we should compare the majorant $\mathscr{M}$ from (25) with the exact error $e := \|\nabla(u - u_{\varepsilon,h})\|_A$ on various meshes. However in these examples the exact solutions are unknown, for this reason we replace it by the so-called "reference" solutions, denoted by u_{ref} and specially computed on a mesh much finer than those used in error estimation tests.

We have computed the values of majorants $\mathscr{M}$, reference errors e_{ref} in the energy norm $\|\cdot\|_A$ as $h \to 0$, and the corresponding efficiency indices i_{eff} defined by the relations

$$e_{ref} := \|\nabla u_{ref} - \nabla u_{\varepsilon,h}\|_A, \quad i_{eff} := \frac{\mathscr{M}}{e_{ref}}. \tag{26}$$

It turns out that for all approximate models the efficiency indices are moderately small (cf. Tables 4 and 5).

$-\log_2 h$	t_{sol}, $[sec]$	t_{maj}, $[sec]$	Model 1			Model 2		
			$\mathscr{M}$	e_{ref}	i_{eff}	$\mathscr{M}$	e_{ref}	i_{eff}
3	0.251	0.333	0.0605	0.0313	1.93	0.0556	0.0294	1.89
4	0.346	0.392	0.0394	0.0196	2.01	0.0352	0.0161	2.19
5	0.938	1.031	0.0282	0.0153	1.84	0.0243	0.0103	2.36
6	2.221	3.982	0.0226	0.0138	1.64	0.0192	0.0079	2.43
7	8.930	15.612	0.0203	0.0136	1.49	0.0168	0.0073	2.30

Table 4: *CPU time for the solution of the diffusion equation and approximation of the flux function in seconds and convergence of errors and majorants for Models 1 and 2.*

$-\log_2 h$	Model 3			Model 4			Exact Problem		
	$\mathscr{M}$	e_{ref}	i_{eff}	$\mathscr{M}$	e_{ref}	i_{eff}	$\mathscr{M}$	e_{ref}	i_{eff}
4	0.0334	0.0156	2.14	-	-	-	-	-	-
5	0.0230	0.0093	2.47	0.0224	0.0090	2.49	0.0155	0.0082	1.89
6	0.0175	0.0062	2.82	0.0171	0.0059	2.90	0.0106	0.0049	2.16
7	0.0154	0.0054	2.85	0.0148	0.0049	3.02	0.0082	0.0028	2.93

Table 5: *Convergence of errors and majorants for Models 3, 4 and the exact problem*

We assume that the diffusion problem (1) with the parameters (22)-(23) should be solved for some given accuracy δ. Table 3 shows that, e.g., for $\delta \leq 0.035$ we do not need to solve the exact diffusion problem (1): Solving Model 3 for the mesh with $h = 2^{-4}$, one gets a total error majorant that is smaller than the accuracy δ, spending essentially less CPU time.

One can find the shortest way to choose the optimal model in the previous test, applying the MD**E** strategy from Section 2.2 presented in Figure 6: We choose, e.g., $\alpha = 0.4$ and start with Model 1 on the mesh, corresponding to $h = 2^{-3}$. In this case we get $\mathcal{M} > \delta$ and $E^{\varepsilon_1,}_{mod} < \alpha\, E^{\varepsilon_1,3}_{disc}$ (cf. Figure 5) and should refine the mesh. On the mesh with $h = 2^{-4}$ we obtain $E^{\varepsilon_1,}_{mod} > \alpha\, E^{\varepsilon_1,4}_{disc}$ hence, we should pass to the more accurate Model 2, if the calculated total error majorant exceeds the target accuracy. For Model 2, we have again $E^{\varepsilon_2}_{mod} > \alpha\, E^{\varepsilon_2,4}_{disc}$ and pass to Model 3 etc.

Test 2.2: In the following numerical experiments, we investigate the dependence of $\mathscr{M}$ on the model parameter ε, defined by

$$\varepsilon := \sup_{\widetilde{\omega}\in\widetilde{\mathcal{H}}} \sup_{x\in(\partial\widetilde{\omega}\cap\Omega)} \inf_{y\in\partial\omega_0} \|x - y\|.$$

For the approximate models, we have the following values of ε:

$$\varepsilon_1 = 0.1822,\ \varepsilon_2 = 0.0699,\ \varepsilon_3 = 0.0442,\ \varepsilon_4 = 0.0313.$$

We solve these models for the following three cases of the diffusion coefficients:

1. $A|_{\omega_0} = I \quad \text{and} \quad A|_{\omega_1} = 2\,I$
2. $A|_{\omega_0} = I \quad \text{and} \quad A|_{\omega_1} = 4\,I$
3. $A|_{\omega_0} = I \quad \text{and} \quad A|_{\omega_1} = 10\,I$

From Figure 7 we conclude that $\mathcal{M} = \mathcal{O}(k\,\varepsilon^{\nu})$, where $\nu \in \mathbb{R}$ is constant for the chosen model hierarchy, and $k \in \mathbb{R}$ depends on h and the coefficient $\frac{A|_{\omega_1}}{A|_{\omega_0}}$. In our numerical experiment we approximately get $\nu \approx \frac{2}{15}$.

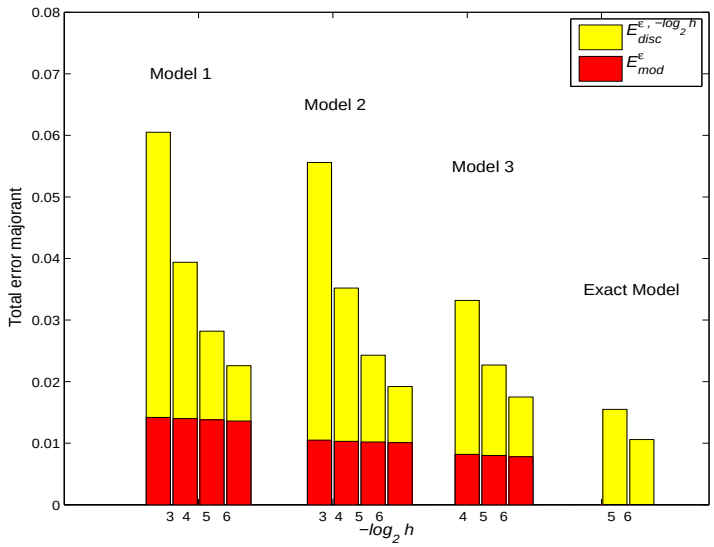

Figure 5: *The absolute values of the total error majorants for the exact and the approximate models.*

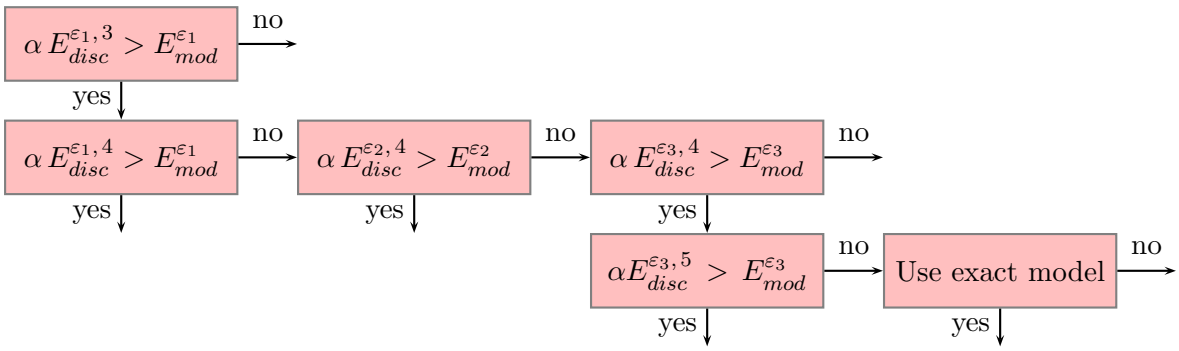

Figure 6: *Combined modelling – discretization error minimization strategy*

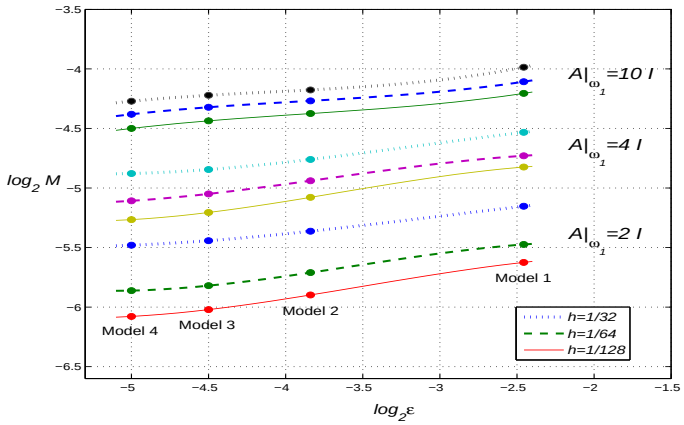

Figure 7: *Logarithmic plot of the convergence rate for the total error majorant with respect to* ε *for the mesh sizes* $h = 2^{-5}$, $h = 2^{-6}$ *and* $h = 2^{-7}$ *and three different cases of diffusion coefficients*

5 Conclusions

We have presented a modelling-discretization strategy for computing approximate solutions of elliptic boundary value problems with complicated structure of the coefficients that form the main part of the differential operator. This strategy is based on the explicit evaluation of discretization and modelling errors. Numerical tests show that in many cases, approximate solutions with a desirable (engineering) accuracy can be obtained by using of rather coarse models, avoiding difficulties arising if the exact resolution of diffusion coefficients is used. Also, the estimates allow us to estimate the errors caused by incomplete knowledge of the coefficients that may arise due to uncertainties in the problem data or errors of numerical integration.

References

[1] Ainsworth, M.: A posteriori error estimation for fully discrete hierarchic models of elliptic boundary value problems on thin domains. Numer. Math., **80**, 325-362 (1998)

[2] Ainsworth, M., Arnold, A: A reliable a posteriori error estimator for adaptive hierarchic modelling. In Adv. Adap. Comp. Meth. Mech., Ladevéze P , Oden JT (eds), 101-114 (1998)

[3] Ainsworth, M., Oden, J.T.: A posteriori error estimation in finite element analysis, Wiley (2000)

[4] Babuška, I., Rheinboldt, W. C.: A posteriori error estimates for the finite element method. Intern. J. Numer. Math. Engrg., **12**, 1597-1615 (1978)

[5] Babuška, I., Rheinboldt, W. C.: Error estimates for adaptive finite element computations. SIAM J. Numer. Anal., **15**, 736-754 (1978)

[6] Babuška, I., Rodríguez, R.: The problem of the selection of an a posteriori error indicator based on smoothing techniques. Internat. J. Numer. Meth. Engrg. ,**36**, 539-567 (1993)

[7] Babuška, I., Schwab, C.: A posteriori error estimation for hierarchic models of elliptic boundary value problems on thin domains. SIAM J. Numer. Anal., **33**, 221–246 (1996)

[8] Carstensen, C., Sauter. S.: A posteriori error analysis for elliptic PDEs on domains with complicated structures. Numer. Math., **96**, 4, 691-721 (2004)

[9] Chipot, M.: Elliptic Equations: An Introductory Course. Birkhäuser Verlag AG (2009)

[10] Clément, Ph.: Approximations by finite element functions using local regularization. RAIRO Anal. Numer., **9**, R-2, 77-84 (1975)

[11] Dörfler, W., Rumpf, M.: An adaptive strategy for elliptic problems including a posteriori controlled boundary approximation. Math. Comput., **67**, 224, 1361-1382 (1998)

[12] Neittaanmäki, P., Repin, S. I.: Reliable methods for computer simulation. Error control and a posteriori estimates. Elsevier, New York (2004)

[13] Repin, S.: A posteriori error estimation for nonlinear variational problems by duality theory. Zapiski Nauch. Semin. (POMI), **243**, 201-214 (1997)

[14] Repin, S.: A posteriori error estimates for Partial Differential Equations. Walter de Gruyter, Berlin (2008)

[15] Repin, S.: A posteriori error estimation for variational problems with uniformly convex functionals. Math. Comp., **69**, 230, 481-500 (2000)

[16] Repin, S., Sauter, S.: Computable estimates of the modeling error related to Kirchhoff-Love plate model. Anal. and Appl., **8**, 4, 1-20 (2010)

[17] Repin, S., Sauter, S., Smolianski, A.: A posteriori error estimation for the Dirichlet problem with account of the error in the approximation of boundary conditions. Computing, **70**, 205-233 (2003)

[18] Repin, S., Sauter, S., Smolianski, A.: Duality Based A Posteriori Error estimator for the Dirichlet Problem. Proc. Appl. Math. Mech., **2**, 513-514 (2003)

[19] Repin, S., Sauter,S., Smolianski,A.: A posteriori estimation of dimension reduction errors for elliptic problems in thin domains. SIAM J. Numer. Anal., **42**, 1435-1451 (2004)

[20] Repin, S., Sauter, S., Smolianski, A.: A Posteriori Control of Dimension Reduction Errors on Long Domains. Proc. Appl. Math. Mech., **4**, 714-715 (2004)

[21] Repin, S., Sauter, S., Smolianski, A.: A posteriori error estimation for the Poisson equation with mixed Dirichlet/Neumann boundary conditions. J. Comput. Appl. Math., **164/165**, 601-612 (2004)

[22] Repin, S., Sauter, S., Smolianski, A.: Two-Sided A Posteriori Error Estimates for Mixed Formulations of Elliptic Problems. SIAM J. Numer. Anal., **45**, 928-945 (2007)

[23] Repin, S., Valdman, J.: Functional a posteriori error estimates for problems with nonlinear boundary conditions. J. Numer. Math. **16**, 1, 51-81 (2008)

[24] Schwab, C.: A-posteriori modeling error estimation for hierarchic plate model. Numer. Math., **74**, 221-259 (1996)

[25] Verfürth, R.: A review of a posteriori error estimation and adaptive mesh-refinement techniques, Wiley-Teubner, Amsterdam (1996)

[26] Valdman, J.: Minimization of functional majorant in a posteriori error analysis based on H(div) multigrid-preconditioned CG method. Adv. Numer. Math., Advances in Numerical Analysis, Article ID 164519 (2009)

[27] Vogelius, M., Babuška, I. (1981): On a dimensional reduction method I. The optimal selection of basis functions. Math. Comp., **37**, 31–46